

XY-Ashkin-Teller Phase Diagram in d=3

Alpar Türkoğlu^{1,2} and A. Nihat Berker^{3,4,5}

¹Department of Physics, Boğaziçi University, Bebek, İstanbul 34342, Turkey

²Department of Electrical and Electronics Engineering,
Boğaziçi University, Bebek, İstanbul 34342, Turkey

³Faculty of Engineering and Natural Sciences, Kadir Has University, Cibali, İstanbul 34083, Turkey

⁴TÜBİTAK Research Institute for Basic Sciences, Gebze, Kocaeli 41470, Turkey

⁵Department of Physics, Massachusetts Institute of Technology, Cambridge, Massachusetts 02139, USA

The phase diagram of the Ashkin-Tellerized XY model in spatial dimension $d = 3$ is calculated by renormalization-group theory. In this system, each site has two spins, each spin having orientation continuously varying in 2π radians. Nearest-neighbor sites are coupled by the two-spin and four-spin interactions. The model has a quasi-disorder line along which actually no ordering occurs. The phase diagram has ordered phases that are ferromagnetic and antiferromagnetic in each of the spins, and phases that are ferromagnetic and antiferromagnetic in the multiplicative spin variable. The renormalization-group flows are in terms of the doubly composite Fourier coefficients of the exponentiated energy of nearest-neighbor spin separations. The values of these Fourier coefficients at the fixed points that attract the ordered phases indicate that, in this $d = 3$ system, the ordered phases are algebraically ordered.

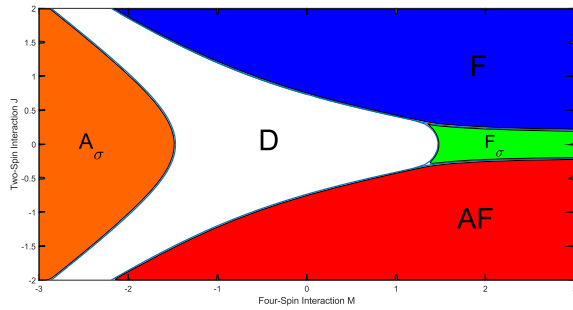


FIG. 1. Calculated phase diagram of the XY Ashkin-Teller model. The ferromagnetic (F) and antiferromagnetic (A) phases of the continuously orientable spin variables \vec{s}_i and \vec{t}_i , and the ferromagnetic (F_σ) and antiferromagnetic (A_σ) phases of the composite spin variable $\vec{s}_i \vec{t}_i$, and the disordered phase (D) are shown.

I. CONTINUOUSLY ORIENTABLE SPINS AND ASHKIN-TELLER COMPLEXITY

The conventional Ashkin-Teller model is a doubled-up Ising model, ushering a multiplicity of order parameters and ordered phases from this discrete-spin model. Using continuously orientable XY spins, instead of discrete Ising spins, brings even more interest. The resulting model is defined by the Hamiltonian

$$\begin{aligned} -\beta\mathcal{H} = \sum_{\langle ij \rangle} [J(\vec{s}_i \cdot \vec{s}_j + \vec{t}_i \cdot \vec{t}_j) + M(\vec{s}_i \cdot \vec{s}_j)(\vec{t}_i \cdot \vec{t}_j)], \\ = \sum_{\langle ij \rangle} -\beta\mathcal{H}_{ij}(\vec{s}_i, \vec{t}_i; \vec{s}_j, \vec{t}_j) \quad (1) \end{aligned}$$

where $\beta = 1/k_B T$, at each site i there are two XY unit spins \vec{s}_i, \vec{t}_i that can point in 2π directions, and the sum

is over all interacting quadruples of spins on nearest-neighbor pairs of sites.

II. METHOD: DOUBLE FOURIER EXPANSION OF TWO CONTINUOUS ANGLES

The renormalization-group transformation is done with length rescaling factor $b = 3$ in order to conserve the ferromagnetic-antiferromagnetic symmetry of the method. This method involves decimating three bonds in series into a single bond, followed by superimposing $b^{d-1} = 9$ bonds.

In the first, decimation, step of the renormalization-group transformation, a decimated bond is obtained by integrating over the shared two spins of two bonds. With $u_{ij}(\theta_{ij}, \varphi_{ij}) = e^{-\beta\mathcal{H}_{ij}(\vec{s}_i, \vec{t}_i, \vec{s}_j, \vec{t}_j)}$ being the exponentiated nearest-neighbor Hamiltonian between sites (i, j) , and $\theta_{ij} = \theta_i - \theta_j$ and $\varphi_{ij} = \varphi_i - \varphi_j$ being the angles between the planar unit vectors (\vec{s}_i, \vec{s}_j) and (\vec{t}_i, \vec{t}_j) , decimation proceeds as

$$\tilde{u}_{13}(\theta_{13}, \varphi_{13}) = \int_0^{2\pi} u_{12}(\theta_{12}, \varphi_{12}) u_{23}(\theta_{23}, \varphi_{23}) \frac{d\theta_2}{2\pi} \frac{d\varphi_2}{2\pi}. \quad (2)$$

Using the double Fourier transformation

$$\begin{aligned} f(k, l) &= \int_0^{2\pi} u(\theta, \varphi) e^{ik\theta+il\varphi} \frac{d\theta}{2\pi} \frac{d\varphi}{2\pi}, \\ u(\theta, \varphi) &= \sum_{k=-\infty}^{\infty} \sum_{l=-\infty}^{\infty} e^{-ik\theta-il\varphi} f(k, l), \quad (3) \end{aligned}$$

the decimation of Eq.(2) becomes

$$\tilde{f}_{13}(k, l) = f_{12}(k, l) f_{23}(k, l). \quad (4)$$

In the second, bond-moving, step of the

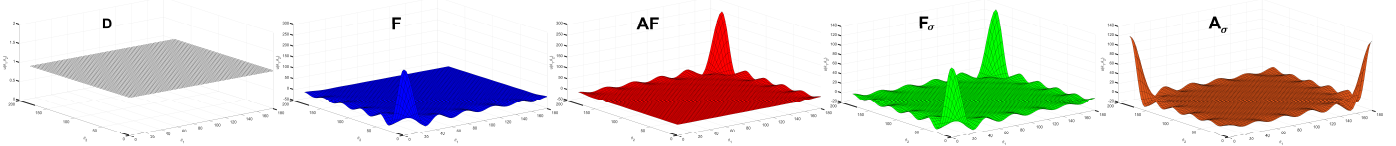


FIG. 2. Renormalization-group sinks of the phases of the XY Ashkin-Teller model. The exponentiated nearest-neighbor energy $u_{ij} = e^{-\beta \mathcal{H}_{ij}(\vec{s}_i, \vec{t}_i; \vec{s}_j, \vec{t}_j)}$ is shown, as a function of the angle θ between the spins \vec{s}_i, \vec{s}_j and the angle φ between the spins \vec{t}_i, \vec{t}_j . The energies are normalized to the maximum value of $u = 1$ by the inclusion of an additive constant to the energy. Diagonal (and cross-diagonal) cross-sections are shown in Fig. 3.

renormalization-group transformation, a bond moving is effected as

$$\begin{aligned} u'_{ij}(\theta, \varphi) &= \tilde{u}_{i_1 j_1}(\theta, \varphi) + \tilde{u}_{i_2 j_2}(\theta, \varphi), \\ f'_{ij}(k, l) &= \sum_{m=-\infty}^{\infty} \sum_{n=-\infty}^{\infty} \tilde{f}_{i_1 j_1}(k-m, l-n) \tilde{f}_{i_2 j_2}(m, n). \end{aligned} \quad (5)$$

We have followed the renormalization-group flows in terms of the $k = 0$ to 30 and $l = 0$ to 30 double Fourier components, also using $f_{ij}(k, l) = f_{ij}(-k, l) =$

$f_{ij}(k, -l) = f_{ij}(-k, -l)$ and setting $f(00)$ by the normalization condition

$$1 = u(0, 0) = \sum_{k=-\infty}^{\infty} \sum_{l=-\infty}^{\infty} f(k, l). \quad (6)$$

III. RESULTS

ACKNOWLEDGMENTS

Support by the Academy of Sciences of Turkey (TÜBA) is gratefully acknowledged.

-
- [1] D. P. Belanger, A. R. King, and V. Jaccarino, Random-field effects on critical behavior of diluted Ising antiferromagnets, *Phys. Rev. Lett.* **48**, 1050 (1982).
 - [2] P.-Z. Wong and J. W. Cable, Hysteretic behavior of the diluted random-field Ising system $Fe_{0.70}Mg_{0.30}Cl_2$, *Phys. Rev. B* **28**, 5361 (1983).
 - [3] A. N. Berker, Ordering under random fields: Renormalization-group arguments, *Phys. Rev. B* **29**, 5243 (1984).
 - [4] H. Yoshizawa, R. A. Cowley, G. Shirane, R. J. Birgeneau, H. J. Guggenheim, and H. Ikeda, Random-field effects in two- and three-dimensional Ising antiferromagnets, *Phys. Rev. Lett.* **48**, 438 (1982).
 - [5] M. S. Cao and J. Machta, Migdal-Kadanoff study of the random-field Ising model, *Phys. Rev. B* **48**, 3177 (1993).
 - [6] A. Falicov, A. N. Berker, and S. R. McKay, Renormalization-group theory of the random-field Ising model in 3 dimensions, *Phys. Rev. B* **51**, 8266 (1995).
 - [7] A. Aharony, Y. Imry, and S.-k. Ma, Lowering of dimensionality in phase transitions with random fields, *Phys. Rev. Lett.* **37**, 1364 (1976).
 - [8] A. A. Migdal, Phase transitions in gauge and spin lattice systems, *Zh. Eksp. Teor. Fiz.* **69**, 1457 (1975) [Sov. Phys. JETP **42**, 743 (1976)].
 - [9] L. P. Kadanoff, Notes on Migdal's recursion formulas, *Ann. Phys. (N.Y.)* **100**, 359 (1976).
 - [10] J. V. José, L. P. Kadanoff, S. Kirkpatrick, and D. R. Nelson, Renormalization, vortices, and symmetry-breaking perturbations in two-dimensional planar model, *Phys. Rev. B* **16**, 1217 (1977).
 - [11] E. Tunca and A. N. Berker, Renormalization-group theory of the Heisenberg model in d dimensions, *Physica A* **608**, 128300 (2022).
 - [12] K. Akin and A. N. Berker, Lower-critical dimension of the random-field XY model and the zero-temperature critical line, *Phys. Rev. E* **106**, 014151 (2022).
 - [13] B. Atalay and A. N. Berker, A lower lower-critical spin-glass dimension from quenched mixed-spatial-dimensional spin glasses, *Phys. Rev. E* **98**, 042125 (2018).
 - [14] E. Tunca and A. N. Berker, Nematic ordering in the Heisenberg spin-glass system in d=3 dimensions, *Phys. Rev. E* **107**, 014116 (2023).
 - [15] S. R. McKay, A. N. Berker, and S. Kirkpatrick, Spin-glass behavior in frustrated Ising models with chaotic renormalization-group trajectories, *Phys. Rev. Lett.* **48**, 767 (1982).
 - [16] S. R. McKay, A. N. Berker, and S. Kirkpatrick, Amorphously packed, frustrated hierarchical models: Chaotic rescaling and spin-glass behavior, *J. Appl. Phys.* **53**, 7974 (1982).
 - [17] A. N. Berker and S. R. McKay, Hierarchical models and chaotic spin glasses, *J. Stat. Phys.* **36**, 787 (1984).
 - [18] M. Hinczewski and A.N. Berker, Finite-temperature phase diagram of nonmagnetic impurities in high-temperature superconductors using a d=3 tJ model with quenched disorder, *Phys. Rev. B* **78**, 064507 (2008).
 - [19] K. Hui and A. N. Berker, Random-field mechanism in random-bond multicritical systems, *Phys. Rev. Lett.* **62**, 2507 (1989).
 - [20] K. Hui and A. N. Berker, erratum, *Phys. Rev. Lett.* **63**, 2433 (1989).
 - [21] B. Nienhuis, A.N. Berker, E.K. Riedel, and M. Schick, First- and second-order phase transitions in Potts models: Renormalization-group solution, *Phys. Rev. Lett.*

- 43**, 737 (1979).
- [22] D. Andelman and A. N. Berker, q-State Potts models in d-dimensions: Migdal-Kadanoff approximation, *J. Phys. A* **14**, L91 (1981).
- [23] H. Y. Devre and A. N. Berker, First-order to second-order phase transition changeover and latent heats of q-state Potts models in d=2,3 from a simple Migdal-Kadanoff adaptation, *Phys. Rev. E* **105**, 054124 (2022).
- [24] E. C. Artun and A. N. Berker, Complete density calculations of q-state Potts and clock models: Reentrance of interface densities under symmetry breaking, *Phys. Rev. E* **102**, 062135 (2020).
- [25] A. N. Berker and S. Ostlund, Renormalisation-group calculations of finite systems: Order parameter and specific heat for epitaxial ordering, *J. Phys. C* **12**, 4961 (1979).
- [26] R. B. Griffiths and M. Kaufman, Spin systems on hierarchical lattices: Introduction and thermodynamic limit, *Phys. Rev. B* **26**, 5022R (1982).
- [27] M. Kaufman and R. B. Griffiths, Spin systems on hierarchical lattices: 2. Some examples of soluble models, *Phys. Rev. B* **30**, 244 (1984).
- [28] J. Clark and C. Lochridge, Weak-disorder limit for directed polymers on critical hierarchical graphs with vertex disorder, *Stochastic Processes Applications* **158**, 75 (2023).
- [29] M. Kotorowicz and Y. Kozitsky, Phase transitions in the Ising model on a hierarchical random graph based on the triangle, *J. Phys. A* **55**, 405002 (2022).
- [30] P. P. Zhang, Z. Y. Gao, Y. L. Xu, C. Y. Wang, and X. M. Kong, Phase diagrams, quantum correlations and critical phenomena of antiferromagnetic Heisenberg model on diamond-type hierarchical lattices, *Quantum Science Technology* **7**, 025024 (2022).
- [31] K. Jiang, J. Qiao, and Y. Lan, Chaotic Renormalization Flow in the Potts model induced by long-range competition, *Phys. Rev. E* **103**, 062117 (2021).
- [32] G. Mograby, M. Derevyagin, G. V. Dunne, and A. Teplyakov, Spectra of perfect state transfer Hamiltonians on fractal-like graphs, *J. Phys. A* **54**, 125301 (2021).
- [33] I. Chio, R. K. W. Roeder, Chromatic zeros on hierarchical lattices and equidistribution on parameter space, *Annales de l'Institut Henri Poincaré D*, **8**, 491 (2021).
- [34] B. Steinhurst and A. Teplyakov, Spectral analysis on Barlow and Evans' projective limit fractals, *J. Spectr. Theory* **11**, 91 (2021).
- [35] A. V. Myshlyavtsev, M. D. Myshlyavtseva, and S. S. Akinmenko, Classical lattice models with single-node interactions on hierarchical lattices: The two-layer Ising model, *Physica A* **558**, 124919 (2020).
- [36] M. Derevyagin, G. V. Dunne, G. Mograby, and A. Teplyakov, Perfect quantum state transfer on diamond fractal graphs, *Quantum Information Processing*, **19**, 328 (2020).
- [37] S.-C. Chang, R. K. W. Roeder, and R. Shrock, q-Plane zeros of the Potts partition function on diamond hierarchical graphs, *J. Math. Phys.* **61**, 073301 (2020).
- [38] C. Monthus, Real-space renormalization for disordered systems at the level of large deviations, *J. Stat. Mech. - Theory and Experiment*, 013301 (2020).
- [39] O. S. Sariyer, Two-dimensional quantum-spin-1/2 XXZ magnet in zero magnetic field: Global thermodynamics from renormalisation group theory, *Philos. Mag.* **99**, 1787 (2019).
- [40] P. Peczak, Alan M. Ferrenberg, and D. P. Landau, High-accuracy Monte Carlo study of the three-dimensional classical Heisenberg ferromagnet, *Phys. Rev. B* **43**, 6087 (1991).
- [41] P. E. Cladis, New liquid-crystal phase diagram, *Phys. Rev. Lett.* **35**, 48 (1975).
- [42] R. R. Netz and A. N. Berker, Smectic C order, in-plane domains, and nematic reentrance in a microscopic model of liquid crystals, *Phys. Rev. Lett.* **68**, 333 (1992).
- [43] J. O. Indekeu, A. N. Berker, C. Chiang, and C. W. Garland, Reentrant transition enthalpies of liquid crystals: The frustrated spin-gas model and experiments, *Phys. Rev. A* **35**, 1371 (1987).
- [44] C. A. Vause and J. S. Walker, Effects of orientational degrees of freedom in closed-loop solubility phase diagrams, *Phys. Lett. A* **90**, 419 (1982).
- [45] R. G. Caflisch, A. N. Berker, and M. Kardar, Reentrant melting of krypton adsorbed on graphite and the helical Potts-lattice-gas model, *Phys. Rev. B* **31**, 4527 (1985).
- [46] E. F. Sarmento and T. Kaneyoshi, Phase transition of transverse Ising model in a random field, *Phys. Rev. B* **39**, 9555 (1989).
- [47] E. Ilker and A. N. Berker, High q-state clock spin glasses in three dimensions and the Lyapunov exponents of chaotic phases and chaotic phase boundaries, *Phys. Rev. E* **87**, 032124 (2013).
- [48] D. R. Yahme, D. Pereira, L. D. C. Jaubert, L. D. Sanjeewa, M. Powell, J. W. Kolis, Guangyong Xu, M. Enjalran, M. J. P. Gingras, and K. A. Ross, Understanding reentrance in frustrated magnets: the case of the Er₂Sn₂O₇ pyrochlore, *Phys. Rev. Lett.* **127**, 277206 (2021).
- [49] A. M. Frassino, D. Kubiznak, R. B. Mann, and F. Simovic, Multiple reentrant phase transitions and triple points in Lovelock thermodynamics, *J. High Energy Phys.* **09**, 080 (2014).
- [50] A. Dehghani, S. H. Hendi, and R. B. Mann, Range of novel black hole phase transitions via massive gravity: Triple points and N-fold reentrant phase transitions, *Phys. Rev. D* **101**, 084026 (2020).